Chapter 7

HIGH-FREQUENCY EFFECTS AND BEAM ADMITTANCE

In Chapter 6 we found that a modulated beam crossing between two electrodes induces an ac current in the external circuit joining the electrodes. If the electron transit time across the gap between the electrodes is small compared with the period of the beam modulation frequency, the induced ac current equals the ac component of the beam current. However, at high frequencies and moderate or low electron velocities, the electron transit time may be an appreciable part of the period of the ac signal. Suppose, for example, that the electron transit time is one half the period of the modulation frequency. In this case one half a cycle of the modulated beam lies between the electrodes at any instant. Since the induced current is a sum of contributions from the moving electrons in each volume element between the electrodes and since the phase of the beam modulation varies over the distance between the electrodes, the contributions to the induced current are not all in phase, and consequently the total induced current is less than the ac beam current.

Consider a modulated beam crossing between the screen grid and anode of a tetrode or between the grid and anode of a grounded-grid triode. If the modulation frequency is sufficiently high that the electron transit time is comparable with the period of the signal, the ac induced current flowing in the external circuit is less than the ac beam current, and the tube transconductance is correspondingly reduced. In general, at frequencies sufficiently high that electron transit-time effects are important, the transconductance and other tube parameters become complex numbers instead of real numbers, and their magnitudes are functions of the signal frequency.

Suppose an unmodulated beam passes through two grids. If an ac signal is applied between the grids, the electrons are acted on by the ac field, and their velocity acquires an ac component. Each electron in transit between

the grids induces a current proportional to its velocity in the external circuit joining the grids and hence in the signal generator. Since the total induced current is a sum of contributions by the individual electrons in transit between the grids and since the electron velocities have an ac component, the total induced current has an ac component. Furthermore, because the electrons have inertia, the ac component of their velocity is generally not in phase with the applied signal, and the ac induced current is likewise not in phase with the applied signal. The ratio of the ac induced current flowing through the signal generator to the ac voltage applied to the grids is called the *beam admittance* or beam loading. Beam admittance effects become important at high frequencies where the electron transit time is comparable with the period of the ac signal. The small-signal beam admittance is directly proportional to the dc beam current. Generally it has both a conductive and a susceptive part.

In Chapter 6 we noted that the capacitance between the control grid and anode in a grounded-cathode amplifier stage causes a capacitive loading of the input circuit. At high frequencies a conductive loading of the input circuit also occurs in grounded-cathode stages. This is caused partly by the inductance in the cathode lead and partly by beam admittance. At signal frequencies where input conductance first becomes important, the total input conductance is approximately proportional to the product of the low-frequency transconductance of the tube and the square of the signal frequency.

High input conductance is a principal limitation of the performance of high-frequency grounded-cathode amplifiers and oscillators. In some tubes, input conductance limitations become important at frequencies of the order of a few tens of megacycles. However, by using very short cathode leads, and sometimes multiple cathode leads, the cathode lead inductance can be reduced, and the useful operating frequency raised. Similarly, short electrode spacings and high electrode voltages help to increase the operating range by reducing the electron transit times. The electron transit time across the cathode-control grid region can be reduced by locating the plane of the grid wires close to the potential minimum and by using a higher voltage at the grid plane and hence a higher cathode current density.

Still another increase in the input admittance takes place when series resonance occurs between the inductance in the cathode and control grid leads and the capacitance between the cathode and control grid. In designing high-frequency grid-controlled tubes, care must be taken that the frequency of this resonance is well above the operating range.

Generally tubes in which the electrode connections are brought out through the base are useful only at frequencies below 100 Mc, or perhaps a few hundred megacycles in exceptional cases. If operation at still higher

frequencies is needed, planar electrodes are used, and the electrode connections are brought out radially by means of disc leads which pass through the envelope. In this way the lead inductance and rf losses in the leads can be reduced to a minimum.

The chapter concludes with a description of two tubes designed for operation at frequencies well above 100 Mc.

7.1 Electron Transit Time and Beam Admittance

When the electron transit time between the electrodes of a tube is comparable with the period of the ac signal applied to the electrodes, the tube behavior can be modified in several important ways. In this section we consider under separate headings three examples which illustrate these effects.

(*a*) *A Modulated Beam Passing Between Two Electrodes*

As a starting point, it will be helpful to consider the dimensions, beam voltages, and frequencies that are likely to be involved in problems in which transit-time effects are important. Suppose an electron beam is accelerated from zero velocity through 100 volts and then passes at constant velocity through two grids separated by 1 mm. The electron velocity is 5.93×10^6 meters/sec, and the transit time from one grid to the other is $(1/5.93) \times 10^{-9}$ sec. This time is equal to the period of a 5930-Mc signal. If the beam current were modulated at this frequency, one whole cycle of the modulated beam would be between the grids at any instant. If the grids were spaced by 1 cm, the electron transit time would equal the period of a 593-Mc signal.

Let us proceed to determine the current induced in the external circuit

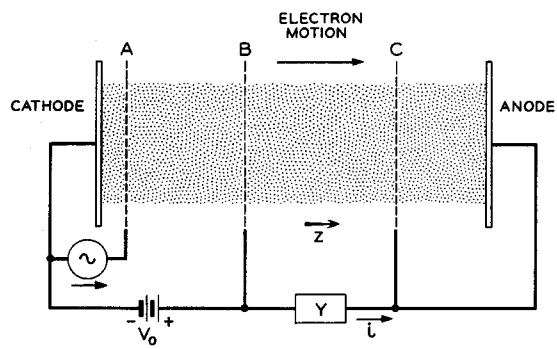

FIG. 7.1-1 The beam passing through grids B and C is modulated by an ac signal applied to grid A.

joining two grids when a modulated beam passes between the grids. A suitable electrode arrangement is shown schematically in Figure 7.1-1. The current of electrons drawn from a planar cathode is modulated by an ac voltage applied to grid A. The electrons are then accelerated through a potential rise V_o and pass at nearly uniform velocity between grids B and C. Finally, they are collected by a planar anode. An admittance Y is connected between grids B and C. It is assumed that the ac voltage developed across this admittance is small compared with the voltage V_o. It is further assumed that grids B and C are ideal electrostatic shields, so that electric fields on one side of the grids do not penetrate through the grids to the other side.

The results of Chapter 6 tell us that *the current flowing in the admittance Y is determined only by the electron current in the space between grids B and C. The electrons striking the anode cancel positive charges which have flowed to the anode to meet them, but they do not give rise to an additional component of current through the admittance Y.* In fact, the induced current flowing in the admittance Y would be no different if grid C were replaced by the anode.

Equation (6.1-8) indicates that the ac current flowing in the admittance Y is given by

$$i(t) = -\int_{\text{volume}} \mathbf{J}(x,y,z,t) \cdot \mathbf{E}_1 dxdydz \tag{7.1-1}$$

where $\mathbf{J}(x,y,z,t)$ is the instantaneous ac current density at the volume element $dxdydz$, and $\mathbf{E}_1$ is a vector function of position discussed in Section 6.1. The integral is taken over the volume of the beam between grids B and C. If the grids extend well beyond the edge of the beam on all sides, $\mathbf{E}_1$ within the beam is normal to the plane of the grids, it is directed from grid B toward grid C, and it is equal in magnitude to $1/d$, where d is the spacing between the grids. Let the electron velocity corresponding to the beam voltage V_o be u_o, and let the direction normal to the plane of the electrodes be the z direction. We shall assume that the magnitude of $\mathbf{J}$ can be expressed as $J_1(x,y) \sin \omega(t - z/u_o)$, and that $\int J_1(x,y)dxdy = I_1$, where the integral is taken over the beam cross section. Substituting for $\mathbf{E}_1$ and $\int J_1(x,y)dxdy$ in Equation (7.1-1), and assuming that $\mathbf{J} \cdot \mathbf{E}_1$ is a *negative* quantity, we obtain

$$\begin{aligned} i(t) &= \frac{I_1}{d} \int_0^d \sin \omega\left(t - \frac{z}{u_o}\right) dz \\ &= \frac{I_1}{d} \frac{u_o}{\omega}\left[\cos\left(\omega t - \frac{\omega d}{u_o}\right) - \cos \omega t\right] \end{aligned} \tag{7.1-2}$$

where distance z is assumed to be measured from grid B toward grid C. If we set $(\omega t - \omega d/2u_o) = A$, and $\omega d/2u_o = B$, the part of Equation (7.1-2)

in brackets can be written in the form cos $(A - B)$ − cos $(A + B)$. Then using the identity that cos $(A - B)$ − cos $(A + B)$ = 2 sin A sin B, we can write Equation (7.1-2) as

$$i(t) = I_1 \frac{\sin \frac{\omega d}{2u_o}}{\frac{\omega d}{2u_o}} \sin \omega\left(t - \frac{d}{2u_o}\right) \tag{7.1-3}$$

Finally, the electron transit time T_o between grids B and C is equal to d/u_o, so that

$$i(t) = I_1 \frac{\sin \frac{\omega T_o}{2}}{\frac{\omega T_o}{2}} \sin \omega\left(t - \frac{T_o}{2}\right) \tag{7.1-4}$$

The factor $[\sin (\omega T_o/2)]/(\omega T_o/2)$ is known as the beam-coupling coefficient, and the angle ωT_o is called the transit angle. The beam-coupling coefficient measures the ratio of the ac current induced in the external circuit to the ac component of the beam current. In subsequent discussion we shall designate this ratio with the letter M. Figure 7.1-2 shows a plot of M as a function of the transit angle ωT_o.

From Equation 7.1-4 we see that the phase of the induced current flowing in the external circuit is the same as that of the beam current at a point midway between the grids.

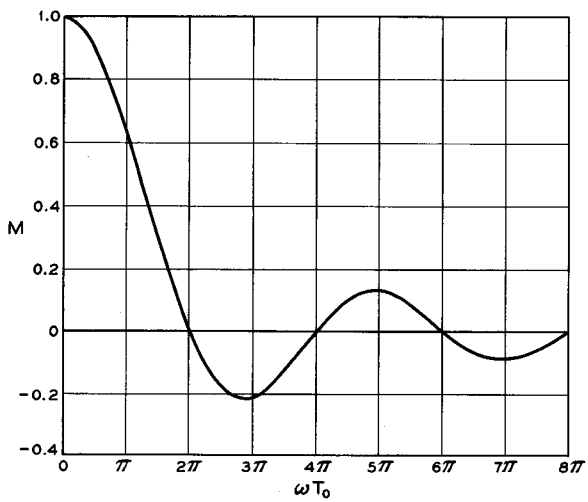

FIG. 7.1-2 The beam-coupling coefficient M plotted as a function of ωT_o.

Consider a tetrode amplifier stage in which the screen grid and anode are operated at the same voltage, and there is little potential depression between the screen grid and anode. The effect of a non-zero transit angle for the screen-grid to anode space is that the magnitude of the current generated by the constant current generator of the equivalent network is multiplied by the factor M and hence is given by $| Mg_m V_g |$.

In the 448A tetrode, described in Section 5.3, the screen grid and anode are operated at 125 volts, and the spacing between these electrodes is 0.5 cm. If the beam current is reduced so that there is little potential depression between the electrodes, the transit angle ωT_o is equal to $4.74 \times 10^{-9} f$ radians, where f is the signal frequency in cycles per second. At a frequency of 1320 Mc, $\omega T_o = 2\pi$, and from Figure 7.1-2 we see that the beam-coupling coefficient M is zero. Furthermore at integral multiples of this frequency, ωT_o is an integral multiple of 2π, and the beam-coupling coefficient is again zero. The frequency 1320 Mc corresponds to the reciprocal of the electron transit time for this particular electrode spacing and beam voltage, so that at this frequency there is one whole cycle of the modulated beam between the electrodes at any instant. When the frequency is an integral multiple of 1320 Mc, there is an integral number of cycles of the modulated beam between the electrodes. Since the induced current flowing in the external circuit is a sum of contributions from each volume element between the electrodes, the *total* induced current must be zero when there is an integral number of cycles of the modulated beam between the electrodes.

The 448A is normally operated at frequencies below 100 Mc. Since ωT_o for the screen-grid to anode space of the 448A is equal to 0.15π at a frequency of 100 Mc, it is evident from Figure 7.1-2 that M for this interaction region is nearly equal to unity for frequencies below 100 Mc. However, in designing tubes to operate at frequencies approaching 1000 Mc, transit-time effects in the output region of the tube may be a serious limitation. Notice that for a given ac beam current passing between the screen grid and anode of a tetrode, the electron transit time from the cathode to the screen grid does not affect the *magnitude* of the ac current induced in the output circuit provided the screen grid acts as a good electrostatic shield. However, the *phase* of the output signal is delayed by the finite transit times involved, and consequently the transconductance as defined by Equation (5.2-1) becomes a complex number.

(*b*) *Small-Signal Admittance of an Unmodulated Beam Passing Between Two Grids at Equal Potential*

Suppose an ac signal is applied between two parallel planar grids, and an initially unmodulated electron beam passes through the grids. The motion

of the electrons in the space between the grids varies in response to the applied ac field, and this causes an induced ac current to flow through the signal generator. The ratio of the induced ac current flowing in the external circuit to the ac voltage applied by the signal generator is called the beam admittance, or beam loading.

Let us derive an expression for the small-signal admittance of an unmodulated beam passing between two grids whose dc potentials are equal. A suitable arrangement of electrodes is shown schematically in Figure 7.1-3. The grids are assumed to be ideal electrostatic shields. An electron

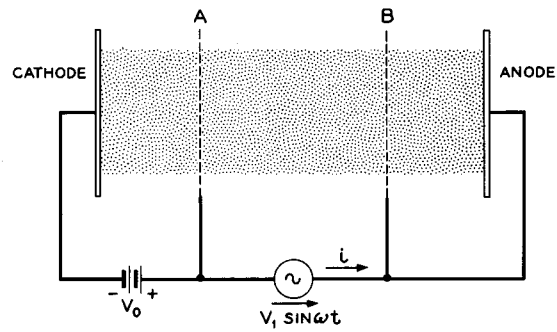

FIG. 7.1-3 The ac voltage applied between grids A and B causes the electron motion to vary in response to the applied field. An induced ac current therefore flows through the signal generator, and the electron beam acts as a load on the signal generator.

beam of current I_o is accelerated through a potential rise V_o before passing through grid A. The space-charge density between the grids is sufficiently low that there is negligible potential depression between the grids. An ac voltage $V_1 \sin \omega t$ is applied between the grids by means of a signal generator. We assume that the signal generator has zero internal impedance for both ac and dc signals and that V_1 is small compared with V_o.

We shall first determine the transit time of an electron which passes from grid A to grid B and is acted on by the ac field $(V_1/d) \sin \omega t$ as it crosses the interelectrode space, where d is the grid spacing. The acceleration of the electron in the region between the grids is given by

$$\frac{d^2z}{dt^2} = \frac{\eta V_1}{d} \sin \omega t = \frac{u_o}{2T_o} \frac{V_1}{V_o} \sin \omega t \tag{7.1-5}$$

where $u_o = \sqrt{2\eta V_o}$ is the velocity of the electrons passing through grid A, and $T_o = d/u_o$ is the electron transit time in the absence of an applied signal. Let the time the electron passed through grid A be t_o. The velocity

of the electron at time t is found by integrating Equation (7.1-5) with respect to time from t_o to t and adding u_o. Thus

$$\frac{dz}{dt} = u_o - \frac{u_o}{2\omega T_o}\frac{V_1}{V_o}(\cos \omega t - \cos \omega t_o) \tag{7.1-6}$$

Integrating once more from t_o to t, we find that the z coordinate of the electron at time t is given by

$$z = u_o(t - t_o) - \frac{u_o}{2\omega^2 T_o}\frac{V_1}{V_o}[\sin \omega t - \sin \omega t_o - \omega(t - t_o)\cos \omega t_o] \tag{7.1-7}$$

where distance z is measured from grid A toward grid B. If we set $z = d$ in this equation, the time t corresponds to the time of arrival of the electron at grid B, and the time $t - t_o$ for $z = d$ is the electron transit time. We shall designate this electron transit time by T. Then

$$d = u_o T - \frac{u_o}{2\omega^2 T_o}\frac{V_1}{V_o}[\sin \omega t - \sin \omega t_o - \omega T \cos \omega t_o] \tag{7.1-8}$$

or

$$T = T_o + \frac{1}{2\omega^2 T_o}\frac{V_1}{V_o}[\sin \omega t - \sin \omega t_o - \omega T \cos \omega t_o] \tag{7.1-9}$$

where we have substituted T_o for d/u_o. Now as $V_1 \to 0$, $T \to T_o$. Since we assume that V_1 is small, the second term on the right-hand side of Equation (7.1-9) is small compared with the first term. We shall use the approximations that $t_o = t - T_o$ and $T = T_o$ in the second term of the right-hand side of the equation. This is equivalent to neglecting terms which involve the product of two or more small quantities. The electron transit time then becomes

$$T = T_o + \frac{1}{2\omega^2 T_o}\frac{V_1}{V_o}[\sin \omega t - \sin \omega(t - T_o) - \omega T_o \cos \omega(t - T_o)] \tag{7.1-10}$$

We can now proceed to determine the current that flows in the external signal generator at time t. This current is a sum of contributions from all electrons in transit between the grids and hence includes all electrons that passed through grid A from time t back to time $t - T$. One electron induces a current $i = \frac{e}{d}\frac{dz}{dt}$ in the external circuit. In an increment of time dt_o an amount of charge $I_o dt_o$ passes through grid A. At time t this charge causes an induced current $\frac{I_o\, dt_o}{d}\frac{dz}{dt}$ to flow in the external circuit, where dz/dt is the velocity of the electrons that comprise the charge $I_o\, dt_o$, and dz/dt is

evaluated at time t. The total induced current flowing in the signal generator therefore is

$$i(t) = \int_{t_0=t-T}^{t_0=t} \frac{I_o}{d}\frac{dz}{dt}dt_o \tag{7.1-11}$$

Substituting for dz/dt from Equation (7.1-6) and carrying out the integration, we obtain

$$i(t) = I_o\frac{T}{T_o} - \frac{I_o}{2(\omega T_o)^2}\frac{V_1}{V_o}[\omega T\cos\omega t - \sin\omega t + \sin\omega(t-T)] \tag{7.1-12}$$

In the first term on the right we can substitute for T from Equation (7.1-10), and in the second term we can use the approximations $t_o = t - T_o$ and $T = T_o$, since the second term is already a small quantity. Thus we obtain

$$i(t) = I_o + V_1\frac{I_o}{2V_o}\left[\frac{2(1-\cos\omega T_o) - \omega T_o\sin\omega T_o}{(\omega T_o)^2}\sin\omega t + \frac{2\sin\omega T_o - \omega T_o(1+\cos\omega T_o)}{(\omega T_o)^2}\cos\omega t\right] \tag{7.1-13}$$

This is of the form $i(t) = I_o + gV_1\sin\omega t + bV_1\cos\omega t$, where

$$g = g_o\frac{2(1-\cos\omega T_o) - \omega T_o\sin\omega T_o}{2(\omega T_o)^2}$$

$$b = g_o\frac{2\sin\omega T_o - \omega T_o(1+\cos\omega T_o)}{2(\omega T_o)^2} \tag{7.1-14}$$

and $g_o = I_o/V_o$. Figure 7.1-4 shows plots of g/g_o and b/g_o.

Equation (7.1-13) shows that the current flowing in the signal generator due to the presence of the beam is made up of a dc term equal to the dc beam current and two ac terms, one in phase with the applied voltage and one in quadrature with the applied voltage. The capacitance between the grids also shunts the voltage generator, and an *additional* current is drawn from the signal generator to charge this capacitance. An equivalent network for the system is shown in Figure 7.1-5. The capacitance C_o is the capacitance between the grids in the absence of the beam. Positive b corresponds to a capacitative susceptance, and negative b corresponds to an inductive susceptance. The admittance $g + jb$ is called the beam admittance or beam loading. It shunts any external circuit connected between the grids. Figure 7.1-4 shows that as ωT_o approaches zero, both g and b go to zero.

In further explanation of the beam admittance, let us return to Equation (7.1-6). Because the electrons are acted on by the applied ac field, their

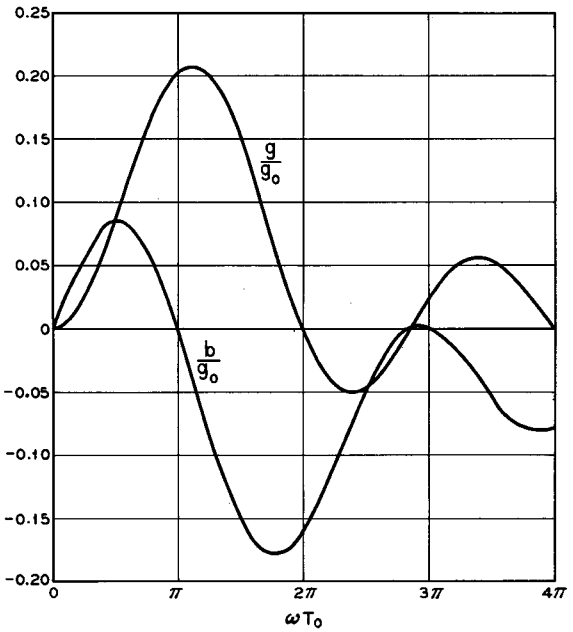

FIG. 7.1-4 The quantities g/g_o and b/g_o plotted as functions of the angle ωT_o.

velocity has an ac component. However, each electron induces a current $i = \frac{e}{d}\frac{dz}{dt}$ in the external circuit, and since dz/dt has an ac component, the induced current resulting from an individual electron has an ac component. When the induced currents from all the electrons in transit between the grids are added together, the resulting total induced current also has an ac component. Furthermore, because the electrons have inertia, the ac component of their velocity is not in phase with the applied field. This accounts for the susceptive part of the beam admittance.

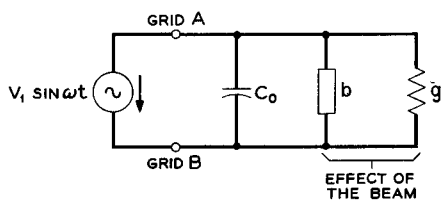

FIG. 7.1-5 An equivalent network for the region between grids A and B in Figure 7.1-3.

To illustrate the magnitudes that might arise from beam-loading effects, consider a 100-volt, 100-ma beam crossing between two grids spaced by 1 cm. We shall assume that the beam current density is sufficiently low that there is negligible potential depression between the grids. If a signal frequency of 200 Mc is applied to the grids, $\omega T_o = 2.11$ radians, and $g + jb = (1.38 + j\,0.78) \times 10^{-4}$ mho. This is equivalent to a resistance of 7200 ohms in parallel with a capacitive reactance of 13,000 ohms. If a parallel resonant circuit were connected between the grids, the beam admittance would change both the tuning and Q of the circuit.

(c) *Impedance of a Space-Charge-Limited Planar Diode*

As a final example of electron transit-time effects, we derive in Appendix X the impedance of a space-charge-limited planar diode. It is assumed in the derivation that the potential minimum coincides with the cathode and that edge effects can be neglected. The impedance of the diode is found to be

$$z = \frac{r}{A} + j\frac{x}{A} \tag{7.1-15}$$

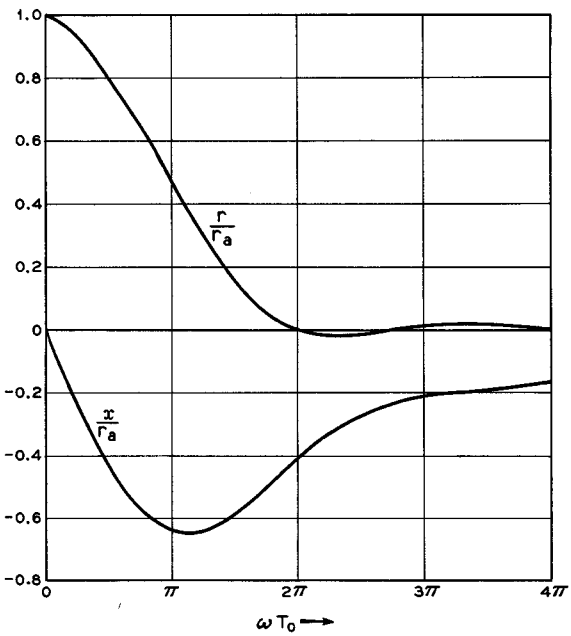

FIG. 7.1-6 The quantities r/r_a and x/r_a plotted as functions of the transit angle ωT_o.

where A is the area of the electrodes, and r and x are given by

$$r = 12r_a\left[\frac{2(1 - \cos \omega T_o) - \omega T_o \sin \omega T_o}{(\omega T_o)^4}\right] \tag{7.1-16}$$

and

$$x = -12r_a\left[\frac{1}{6\omega T_o} + \frac{\omega T_o(1 + \cos \omega T_o) - 2 \sin \omega T_o}{(\omega T_o)^4}\right] \tag{7.1-17}$$

Here T_o is the time required for an electron to travel from the cathode to the anode under the influence of the applied dc field, and ωT_o is the corresponding transit angle. The resistance r_a is the "dynamic anode re-

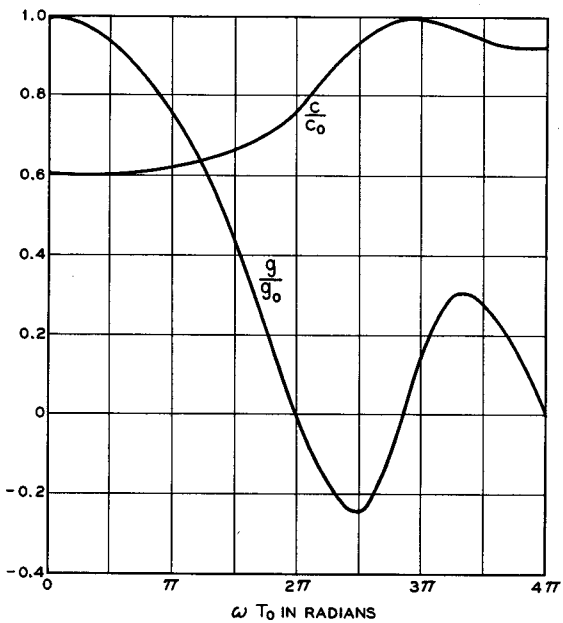

FIG. 7.1-7 The conductance and capacitance of a space-charge-limited planar diode. The conductance g_o is equal to $3J_0A/2V_o$, and the capacitance C_o is equal to the capacitance of the parallel plate capacitor formed by the electrodes in the absence of space charge.

sistance" for a unit area of the diode and is equal to $2V_{ao}/3J_o$, where V_{ao} is the dc voltage applied to the anode, and J_o is the dc current density drawn to the anode. Figure 7.1-6 shows plots of r/r_a and x/r_a as functions of the electron transit angle ωT_o. Figure 7.1-7 shows the conductance and capacitance of the diode as functions of ωT_o.

It is also shown in Appendix X that at *low* frequencies the diode can be represented by an admittance Y such that

$$Y \approx g_o + j\omega\frac{3}{5}C_o \tag{7.1-18}$$

where $g_o = A/r_a$, and C_o is the capacitance of the parallel-plate capacitor formed by the electrodes in the absence of space charge. Thus at low frequencies the capacitance of the diode is *reduced* by the presence of space charge to 3/5 of the diode's capacitance in the absence of space charge. That the capacitance should be *changed* by the space charge is perhaps not surprising if we note that the field distribution and charges on the electrodes are quite different when space charge is present. In fact, when the potential minimum coincides with the cathode, there is no surface charge on the cathode at all. A low-frequency equivalent network for the diode is shown in Figure 7.1-8.

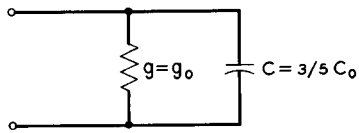

FIG. 7.1-8 A low-frequency equivalent network for a space-charge-limited planar diode.

7.2 The Llewellyn and Peterson Equations

An important contribution to present understanding of the high-frequency electronics of grid-controlled tubes with planar electrodes was made in some studies by Llewellyn and Peterson.[1] We shall not attempt to summarize their paper here but merely show the form of the equations from

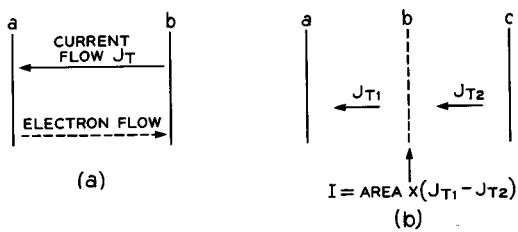

FIG. 7.2-1 (a) The interaction region applicable to Equation (7.2-1). (b) The interaction region bounded by planes a and b is followed by a second interaction region bounded by planes b and c. From J_a, U_a, and J_{T1}, the quantities J_b and U_b can be calculated. These can be used as entrance conditions for the second interaction region, and J_c and U_c can be calculated.

[1]Reference 7a.

which their studies developed. The reader who is interested in pursuing further the subject of high-frequency effects in grid-controlled tubes will find many interesting problems examined in the Llewellyn-Peterson paper.

The approach taken by Llewellyn and Peterson considers the parallel flow of electrons between two planes, a and b, as illustrated in Figure 7.2-1 (a). Plane a might be a cathode or an ideal grid, whereas plane b might be an anode or an ideal grid. Suppose the electron beam passes through plane a with an ac component of convection current density J_a and an ac component of velocity U_a. An ac voltage $V_a - V_b$ is applied between the planes, where $V_a - V_b$ is small compared with the average dc beam voltage in the space between the planes. The electron velocity is assumed to be single-valued over any plane normal to the beam, and the ac component of the electron velocity is small compared with the dc component. The Llewellyn-Peterson equations then take the form:

$$\begin{aligned} V_b - V_a &= A^*J_T + B^*J_a + C^*U_a \\ J_b &= D^*J_T + E^*J_a + F^*U_a \\ U_b &= G^*J_T + H^*J_a + I^*U_a \end{aligned} \tag{7.2-1}$$

where J_b is the ac convection current density at plane b, U_b is the ac component of the electron velocity at plane b, and J_T is the *total* ac beam current density between the planes, that is, the convection current density plus displacement current density, as discussed in Appendix X. Between any two electrodes J_T is a constant, independent of distance from an electrode. If plane b were an anode, then J_T times the area of the beam would be the ac current flowing in the anode lead, edge effects being neglected. The coefficients A^* to I^* are tabulated in Appendix XI. The coefficients are simple functions of the dc electron velocities at planes a and b, the dc transit time for the electrons crossing from plane a to plane b and the corresponding transit angle, and a space charge parameter ζ which varies from 0 with no space charge to 1 with maximum possible space charge. It should be noted that all quantities in Equations (7.2-1) are phasors.

If plane b is followed by a second "interaction region" bounded by planes b and c, as shown in Figure 7.2-1(b), the quantities J_b and U_b, together with the corresponding dc quantities, can be used as entrance conditions for the second region. The total current density in the second region, J_{T2}, is equal to J_{T1} minus the current per unit area flowing into plane b through an external lead. In terms of J_b, U_b, and J_{T2}, the ac convection current density and electron velocity at the third plane, J_c and U_c, can be calculated by further application of Equations (7.2-1).

Now the total current density J_T flowing toward any grid plane or electrode (from both sides) multiplied by the area of the beam equals the ac current flowing away from the electrode in the external lead. Llewellyn

and Peterson used this relationship and the expressions for J_T in the various interaction regions of a multi-electrode tube to construct an equivalent network for such a tube. The network is of particular value in analyzing the high-frequency performance of planar grid-controlled tubes. The equivalent network of a triode operating with the grid negative with respect to the cathode is shown in Figure 7.2-2. Llewellyn and Peterson show that under usual operating conditions the effects of space charge in the region between the control grid and anode can be neglected, and in this case the admittance y_{22} shown in the figure is simply the free-space capacitance C_{22} between the anode and a conducting plane coincident with the grid plane. The capacitance C_g is equal to μC_{22}, where μ is the amplification factor of the tube. (If the grid were an ideal electrostatic shield, μ would be infinitely large, and C_g could be replaced by a direct connection from the grid terminal to the central node of the network.) The admittance y_{11} is the admittance of a space-charge-limited planar diode of spacing equal to the cathode-grid spacing and applied dc voltage equal to the effective beam voltage at the grid. It is the reciprocal of the impedance z given by Equation (7.1-15). At low frequencies the transadmittance y_{12} is approximately equal to minus the low-frequency transconductance of the tube. However, at higher frequencies, it is modified to take into account the effects of the finite transit angles in the cathode-grid region and the grid-anode region. In Reference 7a, Figure 8 shows the effect of frequency on the phase and magnitude of y_{12}.

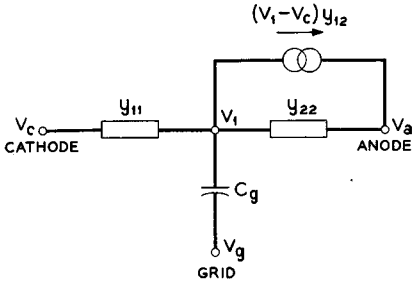

FIG. 7.2-2 The equivalent network for a triode with grid negative with respect to the cathode, as derived by Llewellyn and Peterson.

Some consequences of Llewellyn's and Peterson's work are as follows:

1. The three results presented in Section 7.1 can be obtained directly by the application of Equations (7.2-1) to the particular problems considered. However, the equations are of much more general applicability in the sense that they can be used to solve a variety of similar problems with different dc electrode voltages and different amounts of space charge in the beam.

2. At high frequencies the effects of non-zero transit angles in the various interaction regions of a grid-controlled tube can be evaluated by examination of the appropriate equivalent network.

3. When the transit angles in the input region of a grounded-cathode

amplifier are significantly greater than zero, the electron beam causes a loading of the input circuit. (See Section 7.3(a) for further discussion of this effect.) An expression for this beam loading was derived by Llewellyn and Peterson using the appropriate equivalent network. The expression indicates that at frequencies at which the beam loading first becomes important, the conductive part of the loading is approximately proportional to the product of the low-frequency transconductance and the square of the signal frequency. The derivation assumes that the electrons are emitted from the cathode with zero velocity and hence that the potential minimum coincides with the cathode.

7.3 Input Admittance

At high frequencies a principal limitation of grid-controlled tubes when operated as grounded-cathode amplifiers or oscillators arises from conductive loading of the input circuit. Two effects contribute to the loading: one results from inductance in the cathode lead, and the second results from beam loading. Both contribute a conductive loading which is approximately proportional to the product of the transconductance of the tube and the square of the signal frequency. We consider the effects under separate headings below.

(a) *Lead Inductance Effects*

Although the distance from the socket to the cathode electrode of most grid-controlled tubes is small, often only 1 or 2 cm, the inductance associated with this length of lead can give rise to an important loading of the input circuit. Figure 7.3-1 shows schematically a grid-controlled tube in which the cathode lead inductance is represented by a lumped inductance within the tube. We shall assume that the impedance between the socket and ground is negligible, and we shall neglect the loading which results from the non-zero transit angle in the input region of the tube. The phasor corresponding to the input signal v_i is then given by

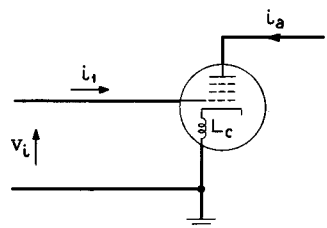

FIG. 7.3-1 Schematic representation of grid-controlled tube with cathode-lead inductance.

$$V_i = V_g + j\omega L_c(I_a + I_1) \quad (7.3\text{-}1)$$

where V_g is the phasor corresponding to the ac voltage between the cathode and grid electrodes, I_a is the phasor corresponding to the current i_a flowing

in the anode circuit, and I_1 is the phasor corresponding to the current i_1 flowing in the input circuit. If the load resistance in the anode circuit is small compared with the dynamic anode resistance, the current flowing in the anode circuit can be expressed as

$$I_a = g_m V_g \tag{7.3-2}$$

where g_m is the transconductance of the tube. If we assume that $I_1 \ll I_a$, Equation (7.3-1) can be written as

$$V_i = V_g(1 + j\omega L_c g_m) \tag{7.3-3}$$

If the input capacitance of the tube is principally that between the control grid and cathode, the voltage V_g is related to the current flowing in the input circuit by

$$V_g = \frac{I_1}{j\omega C_{cg}} \tag{7.3-4}$$

where C_{cg} is the capacitance between the control grid and cathode. Combining Equations (7.3-3) and (7.3-4), we can express the input admittance as

$$Y_i = \frac{I_1}{V_i} = \frac{j\omega C_{cg}}{1 + j\omega L_c g_m} = \frac{j\omega C_{cg}(1 - j\omega L_c g_m)}{1 + \omega^2 L_c^2 g_m^2} \tag{7.3-5}$$

At frequencies of interest the term $\omega^2 L_c^2 g_m^2$ in the denominator is small compared with unity and can be neglected. The input admittance then has a positive real part given by

$$G_i = \omega^2 L_c C_{cg} g_m \tag{7.3-6}$$

This conductance shunts the input circuit, and since it is proportional to the product of L_c and C_{cg}, it is desirable that both of these quantities be as small as possible in tubes used at very high frequencies.

In "miniature" tubes, such as the 403A/6AK5 pentode, described in Section 5.4, low cathode-lead inductance is achieved because of the short distance between the internal electrodes and the pins at the base of the tube. Furthermore, two cathode leads are used in the 403A/6AK5, each connected to separate pins at the tube base. This permits parallel connection at the tube socket and results in a further reduction in the cathode-lead inductance. In the 403A/6AK5, $L_c = 5$ millimicrohenries with parallel connection to the cathode, $C_{cg} = 3.7$ pf (i.e., 3.7×10^{-12} farad), and $g_m = 5 \times 10^{-3}$ mho. Using these values in Equation (7.3-6), we find that at a frequency of 100 Mc, $G_i = 3.6 \times 10^{-5}$ mho. This is equivalent to a shunting resistance of 28,000 ohms at the input of the tube. This resistance is paralleled by the beam-loading conductance discussed in Part (b) below.

In the 448A tetrode, described in Section 5.3, higher transconductance is achieved by the use of a larger cathode area than in the 403A/6AK5 and

a closer cathode-control grid spacing. This increases C_{cg}, and consequently it is even more important to have a low cathode-lead inductance in this tube. For this reason, three separate cathode leads are brought out of the 448A for parallel connection at the base. Measurement of the cathode-lead inductance of the 448A with the three cathode leads in parallel indicates that it is about 4 millimicrohenries. The capacitance C_{cg} is 18 pf, and g_m is 0.034 mho. Substituting these values into Equation (7.3-6), we find that $G_i = 9.7 \times 10^{-4}$ mho at 100 Mc. This is equivalent to a shunting resistance of 1030 ohms across the input circuit.

A second important lead inductance effect in a tube such as the 448A is the fact that series resonance can occur between the inductance of the cathode and control-grid leads and the capacitance between the cathode and control grid. If we assume a total of 10 millimicrohenries inductance in the cathode and control-grid leads in the 448A, series resonance with the 18-pf capacitance between the control grid and cathode occurs at a frequency of 375 Mc. At this frequency the input impedance would be reduced to a very small value.

(*b*) *Beam Loading in Grounded-Cathode Stages*

The beam loading of the input circuit also has a conductive part which at low and moderate frequencies is proportional to the product of the transconductance and the square of the signal frequency. The discussion that follows explains why this is so. Consider a single electron that travels from the cathode to the anode of a grounded-cathode triode. An induced current somewhat like that shown in Figure 7.3-2(b) flows in the external circuit connected between ground and the grid electrode. At time t_o the electron leaves the cathode. At time t_1 it passes the grid, and the direction of the induced current reverses because the direction of the electron velocity relative to the grid plane reverses. At time t_2 the electron strikes the anode. (If the tube were a tetrode or pentode, the time t_2 could be taken as the time at which the electron passes the plane of the screen grid.) The area under the part of the induced current curve from t_o to t_1 equals the area under the part from t_1 to t_2, and if the grid were an ideal electrostatic shield, each area would equal the electronic charge e. At low frequencies, and with many electrons passing the grid per cycle, the current induced in the grid circuit by electrons crossing from the cathode to the grid plane is just balanced by the induced current caused by the electrons crossing from the grid plane to the anode, and there is no net current induced in the grid circuit. However, at higher frequencies, where the electron transit time $T_o = t_2 - t_o$ is a significant part of the period of the ac signal, the induced currents resulting from electrons crossing the two regions may not be exactly 180° out of

phase. As a result, current i_g flows in the grid circuit when a voltage is applied by the signal generator to the grid terminal. The ratio of this ac induced current to the applied signal is called the beam loading admittance.

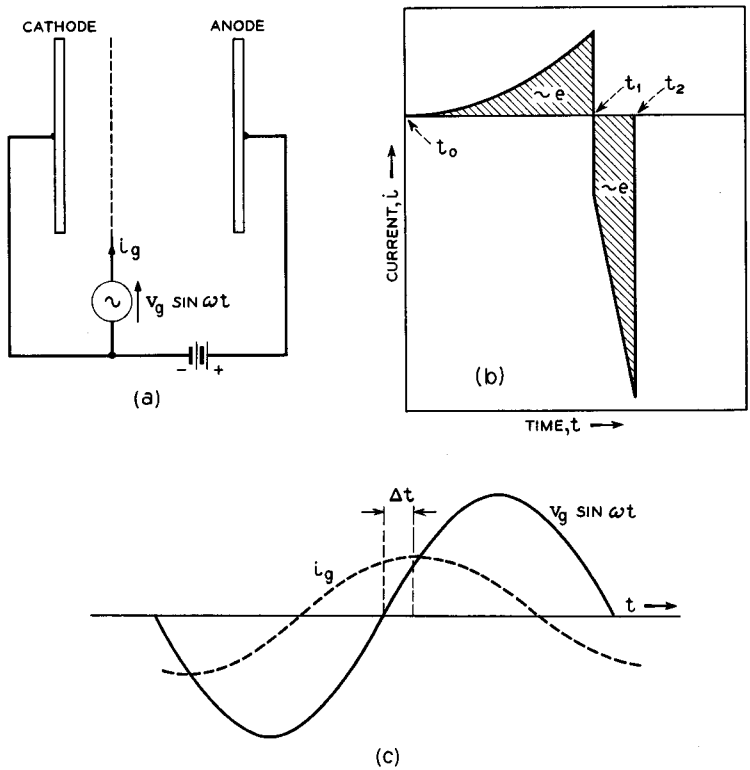

FIG. 7.3-2 The induced current i shown in part b flows in the grid lead when a single electron travels from the cathode to the anode. i_g is the total induced current from all the electrons.

Suppose the ac grid voltage is given by $V_g \sin \omega t$. The ac beam current is then $g_m V_g \sin \omega t$, where g_m is the transconductance of the tube. During the half cycle when the grid voltage is increasing, the current of electrons leaving the cathode (or really the current leaving the potential minimum) is also increasing. We would expect that during most of this half cycle the current induced in the grid circuit by electrons crossing from the cathode to the grid plane would exceed that resulting from electrons crossing from the grid plane to the anode, whereas during the other half cycle the opposite would be the case. Consider the instant when $\sin \omega t = 0$,

and the ac part of the grid voltage is changing from negative to positive. The grid voltage is increasing most rapidly at this instant, and likewise the current of electrons leaving the cathode is increasing most rapidly. Because of the finite transit time $t_1 - t_o$ required for electrons to cross the cathode-grid region, the number of electrons in transit in this region is not maximum at the same instant as the current leaving the cathode is a maximum, but a short time later. Furthermore, the current induced in the grid circuit by an individual electron is essentially zero as the electron leaves the cathode (because the electron velocity is nearly zero), but it increases as the electron approaches the grid plane. For these reasons, *the net current induced in the grid circuit is not maximum when the rate of change of the current leaving the cathode is maximum, but a short time* Δt *later, where* Δt *is an appreciable fraction of* $t_1 - t_o$. Of course, similar reasoning applies to the grid-anode region of the tube and the current induced in the grid circuit by electrons crossing this region. Consequently, the time Δt is actually a function both of $t_1 - t_o$ and $t_2 - t_1$.

From the foregoing discussion, we would expect that the magnitude of the induced grid current i_g would be proportional to the maximum rate of change of the beam current and hence proportional to the product of $g_m V_g$ and the angular frequency ω. Also, for transit times which are small compared with the period of the ac signal, doubling the transit time in the two regions of the tube also doubles the difference between the induced grid currents resulting from electrons crossing the two regions of the tube, and the net induced grid current i_g is doubled. Thus i_g is also proportional to the transit time T_o and can be expressed as

$$i_g = K g_m V_g \omega T_o \cos \omega(t - \Delta t) \tag{7.3-7}$$

where K is a constant. This can be expanded to give

$$i_g = K g_m V_g \omega T_o [\cos \omega t \cos \omega \Delta t + \sin \omega t \sin \omega \Delta t] \tag{7.3-8}$$

The second term in brackets is in phase with the applied grid signal, so that the ratio of this term to the grid voltage $V_g \sin \omega t$ is the conductive part of the input loading. Hence,

$$G_{\text{in}} = K g_m \omega T_o \sin \omega \Delta t \tag{7.3-9}$$

If the electron transit time is small compared with the period of the ac signal, $\omega \Delta t$ is a small angle, and to a first approximation the sine of the angle can be replaced by the angle. Thus

$$G_{\text{in}} \propto g_m \omega^2 T_o \Delta t \tag{7.3-10}$$

It is significant that both the input conductance resulting from cathode-lead inductance and the input conductance resulting from beam loading are proportional to $g_m \omega^2$. Some experimental measurements of the input

loading with grounded-cathode operation are described in Section (c) below.

The input conductance of a *grounded-grid* amplifier stage is high even at relatively low frequencies. From Figure 7.2-2 and the accompanying discussion it can be seen that the input admittance with grounded-grid operation is essentially y_{11} in series with $C_g + C_{22} = C_{22}\ (\mu + 1)$. (We assume the anode is bypassed to ground.) At moderate frequencies the reactance of $C_{22}\ (\mu + 1)$ is negligible, and the input admittance of the amplifier is y_{11}. Now y_{11} is the admittance of a space-charge-limited diode of the same electrode area as the triode, with current density equal to the average beam current density, electrode spacing equal to the cathode-grid spacing, and applied anode voltage equal to the effective beam voltage at the grid. The variation with frequency of the conductive and capacitive parts of this admittance are plotted in Figure 7.1-7. The input conductance of a grounded-grid amplifier stage, therefore, varies as the conductive term plotted in this figure. (We should qualify this statement by noting that the derivation which led to the conductive term plotted in Figure 7.1-7 assumed that the electrons leave the cathode with zero velocity and hence that the potential minimum coincides with the cathode. Actually, it is probable that the electrons which travel part way out to the potential minimum and return to the cathode contribute significantly to the input loading. Furthermore, the derivation does not take into account the Maxwellian distribution of emission velocities, and this also must have an important effect.)

(c) *Some Measurements of the Input Admittance of Grounded-Cathode Amplifier Stages*

When the beam current of a tube is varied by changing the control-

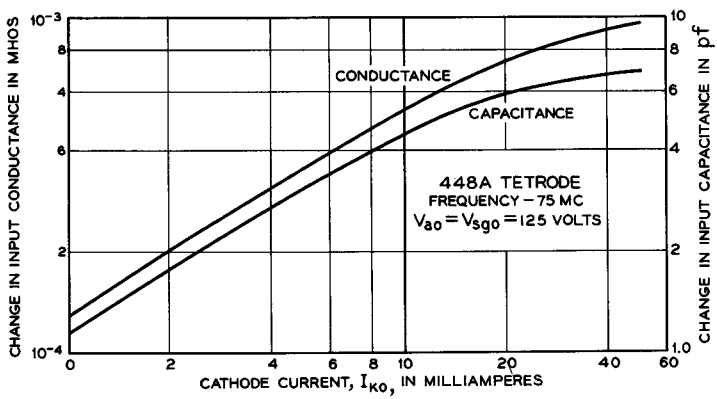

FIG. 7.3-3 Change of input conductance and capacitance with cathode current for the 448A tetrode.

grid voltage, both the input capacitance and input conductance vary. If the control grid is biased negatively to cut off the beam, the input capacitance results only from the interelectrode capacitance plus the capacitance between the leads to the electrodes, and the input conductance

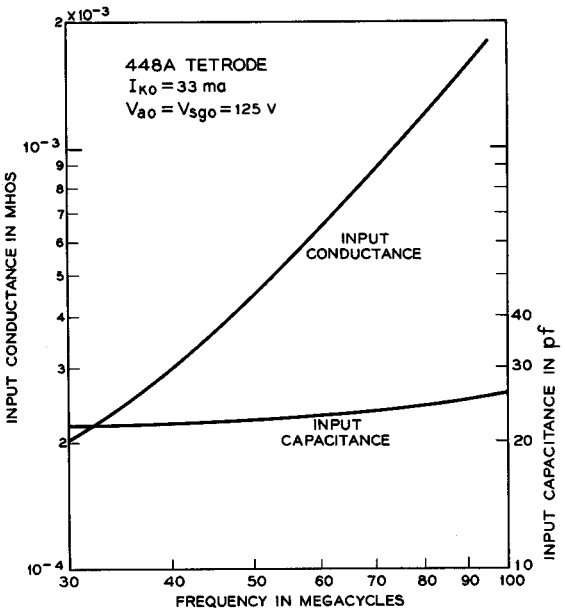

FIG. 7.3-4 Input conductance and input capacitance vs. frequency for the 448A tetrode.

results only from the effects of the series resistance in the leads to the electrodes. However, as the beam current is increased, both the input capacitance and input conductance increase. The increase in input capacitance results from beam loading, whereas the increase in input conductance results from both beam loading and cathode-lead inductance.

Figure 7.3-3 shows the change in input conductance and change in input capacitance vs. beam current for the 448A tetrode, described in Section 5.3. The measurements were made at a frequency of 75 Mc. When the beam is cut off, the input conductance is 1.5×10^{-4} mho, and the input capacitance is 18 pf. Under normal operating conditions, the cathode current is about 35 ma. At this cathode current the input conductance is about 1.03×10^{-3} mho. Figure 7.3-4 shows the variation of input conductance and capacitance with frequency for the 448A. At about 70 Mc the input conductance increases approximately as the square of the signal frequency,

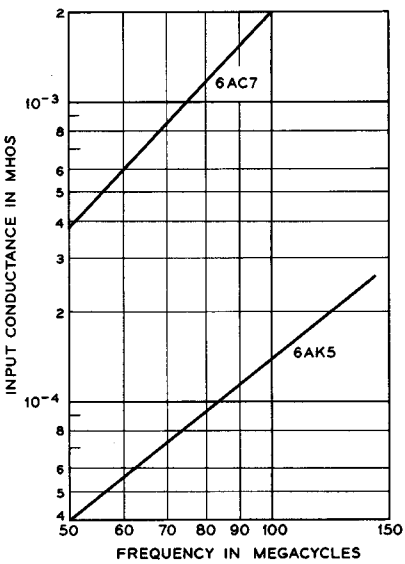

FIG. 7.3-5 Input conductance vs. frequency for the 6AC7 and 6AK5 (Courtesy Radio Corporation of America.)

whereas at lower frequencies it does not increase as rapidly. Figure 7.3-5 shows plots of the input conductance vs. frequency for the 6AC7 and 6AK5 codes. The 6AK5 is described in Section 5.4.

7.4 Two Grid-Controlled Tubes for High-Frequency Amplification

From the discussion given in the previous sections and in Chapter 6, we can list several important electrical and physical characteristics needed in a grid-controlled tube which provides high-gain, broadband amplification at frequencies above 100 Mc/sec:

1. The tube must have a high gain-bandwidth product and hence a high transconductance and low input and output capacitances. This means that the transconductance per unit area of the electrodes must be high, and a short cathode-control grid spacing must be used.

2. The transit angle in the cathode-control grid region must be small so that the input loading (for grounded-cathode operation) is small. The transit angle in the cathode-control grid region can be made small by using a short spacing between the control grid and cathode and a relatively high average voltage at the grid plane and hence a high cathode current density.[2]

3. High voltages and not-too-large electrode spacings must be used at the output interaction gap to reduce the transit angle and keep the beam-coupling coefficient near to unity.

4. The cathode-lead inductance must be small to reduce the input loading, and other lead inductances must be small to prevent the occurrence of series resonance with the interelectrode capacitances.

---

[2]Equation (2) of Appendix X shows that the electron transit time for a planar diode (with potential minimum coincident with the cathode) is proportional to $d^{1/3}/J_o^{1/3}$, where d is the electrode spacing, J_o is the cathode current density. Consequently, the use of a high cathode current density and short cathode-control grid spacing reduces the input transit angle.

Figure 7.4-1 shows the construction of the Bell Telephone Laboratories 1983 tetrode, a developmental tube designed for operation at frequencies of several hundred megacycles per second. The cathode, control grid,

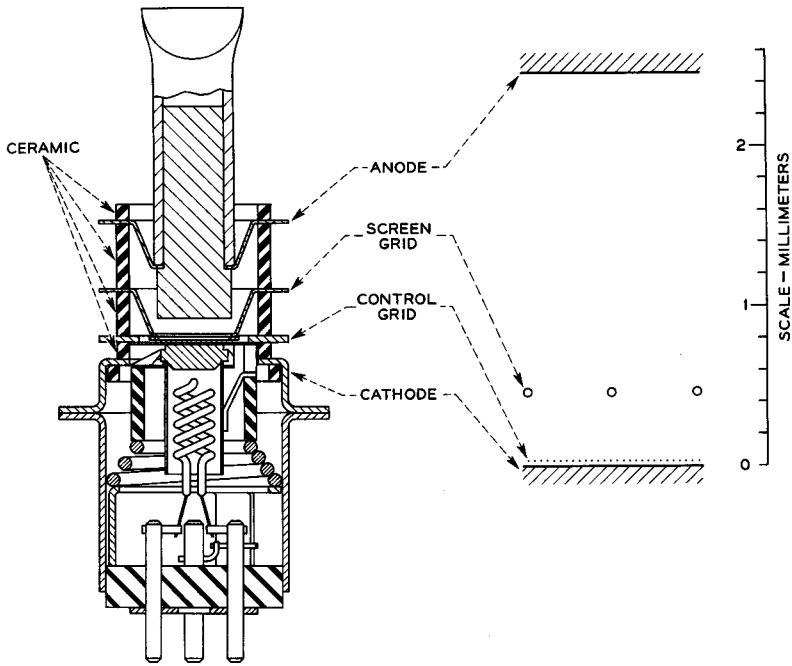

FIG. 7.4-1 The construction of the Bell Telephone Laboratories 1983 tetrode. The overall height of the tube is 5.1 centimeters.

screen grid, and anode connections are brought out radially from the electrodes by means of "disc" leads which are spaced by ceramic rings. The heavy slanted lines in the figure indicate the cross section of the ceramic rings. Vacuum-tight seals are formed between the ceramic rings and the disc leads. This type of envelope construction offers several important advantages:

1. The lead inductance can be made extremely small.
2. At frequencies above 100 Mc/sec, rf losses in wire leads to electrodes become important, and the effects of these losses increase with signal frequency. By using disc leads, the surface area of the leads is greatly increased, and the losses are correspondingly reduced.
3. Power dissipated as heat in the screen grid and anode can be effectively

conducted away, thus increasing the permissible power dissipation within the tube.

Table 5.2-1 lists the operating conditions and important performance characteristics of the 1983 tetrode. A comparison with the 448A tetrode data shows that the high gain-bandwidth product is achieved at the expense of higher cathode current density and reduced cathode-control grid spacing. The transconductance per unit area of the cathode in the 1983 is seven times that of the 448A.

Much more power can be dissipated in the anode of the 1983 than in the anode of the 448A, because the thermal conduction from the anode to the external connections is much better in the 1983. A higher anode voltage can therefore be used, and this helps to reduce the transit angle in the output gap. Also, a smaller spacing between the screen grid and anode is used — 2 mm for the 1983 compared with 5 mm for the 448A. By operating the anode of the 1983 at a voltage well above that of the screen grid, secondary electrons emitted from the anode are prevented from reaching the screen grid. However, part of the primary current to the anode results from secondary emission at the screen grid. To reduce this secondary emission, and in fact to reduce the primary current to the screen grid, a larger screen-grid pitch is used in the 1983, about twice that of the 448A, the screen-grid wire diameter being the same in the two tubes. The heat dissipated in the anode and screen grid of the 1983 is carried away partly by conduction through the external connections to the leads and partly by forced-air cooling.

At the time of writing, a one-stage, grounded-cathode amplifier has been assembled using the 1983. The amplifier has a 50-ohm resistance connected between the control grid and cathode, and a signal generator with a 50-ohm internal impedance is used to drive the amplifier. The amplifier provides a midband gain of 10 db with a 3-db bandwidth extending from 0.5 Mc/sec to 250 Mc/sec. (Note that because of the low input impedance of the stage, only the output capacitance limits the bandwidth in such a stage. Consequently, the gain-bandwidth product given by Equation (6.4-11) is not applicable here.)

The second tube which we shall describe is the Western Electric 416B triode, a tube designed as a grounded-grid amplifier for signal frequencies in the neighborhood of 4000 Mc/sec. The construction of the 416B is illustrated in Figure 7.4-2. The envelope is a metal-and-glass structure in which glass rings separate the anode, grid, and cathode terminals and form vacuum-tight seals with these terminals. The input and output connections to the tube are made by means of waveguides.[3] A cross-sectional view of

[3]See Chapter 8.

the associated waveguide components is shown in Figure 7.4-3. The lower part of the bulb is capacitively coupled to the cathode, and rf connection to the cathode is made through this capacitance. DC connection to the cathode is made through a pin in the base. The electrical characteristics of the 416B are summarized in Table 5.2-1.

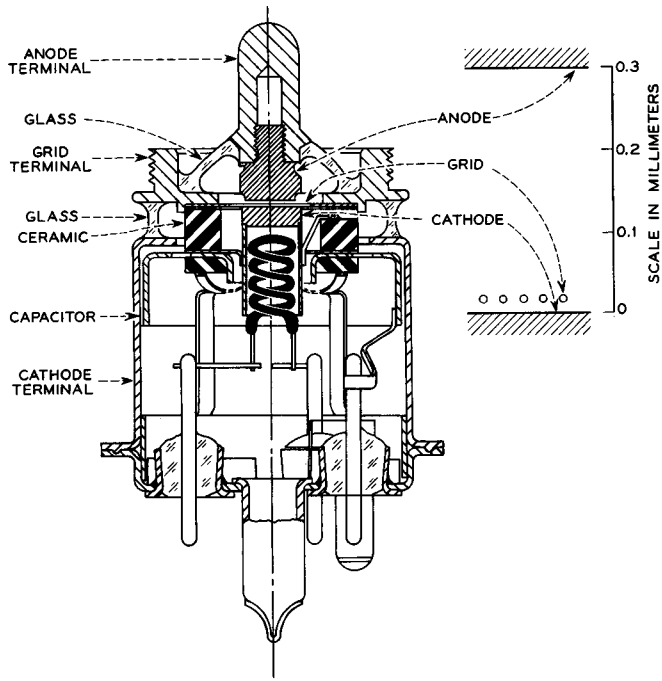

FIG. 7.4-2 The construction of the Western Electric 416B triode. The overall height of the tube is 4.8 cm.

The principal design considerations which led to the electrode structure of the 416B are described in Reference 7c. The design was chosen to obtain as large as possible a product of (midband power gain) × (bandwidth) consistent with practical values of cathode current density and anode and grid power dissipation. (At signal frequencies of 4000 Mc/sec it is more meaningful to use a gain-bandwidth product involving the power gain rather than the voltage gain, since the power gain can be measured directly, whereas the voltage gain must be calculated from measurements of power gain.) Using the equivalent network for a triode given in Figure 7.2-2, the midband power gain with grounded-grid operation can easily be shown to be $|y_{12}|^2/2G_{11}G_o$, where G_{11} is the real part of y_{11}, and G_o is the conductance

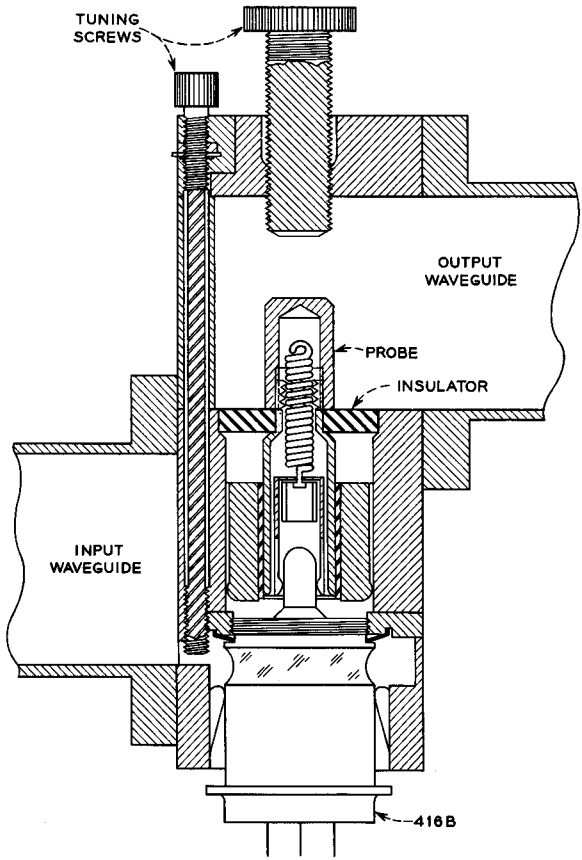

FIG. 7.4-3 The waveguide connections to the 416B. There is effectively a coaxial line from the anode terminal of the tube to a probe which extends into the output waveguide and which acts as a transducer between the coaxial line and the output waveguide.

of the output circuit. We assume here that the characteristic admittance of the output waveguide appears at the tube as an admittance $G_o/2$ and that the losses in the output circuit of the amplifier are adjusted to match this admittance. Hence the total conductance shunting the output circuit is G_o. If is further assumed that the losses in the input circuit contribute a shunting admittance at the input which is small in comparison with G_{11}, and hence the effect of the input losses can be neglected. The capacitance C_g in Figure 7.2-2 is assumed to have negligible reactance at 4000 Mc/sec.

Since the input conductance of a grounded-grid stage is extremely high, the Q of the input circuit is correspondingly low, and the bandwidth of the stage is determined primarily by the output circuit. From Equations (6.4-3) and (6.4-7) the 3-*db bandwidth* of the output circuit is $G_o/2\pi C_o$, where C_o is the capacitance shunting the output circuit. Thus

$$\text{(midband power gain)} \times \text{(3-db bandwidth)} = \frac{|y_{12}|^2}{4\pi G_{11} C_o} \qquad (7.4\text{-}1)$$

The power gain decreases with increasing transit angle in the cathode-grid region, and accordingly a high cathode current density and extremely small cathode-grid spacing are used to minimize the input transit angle.

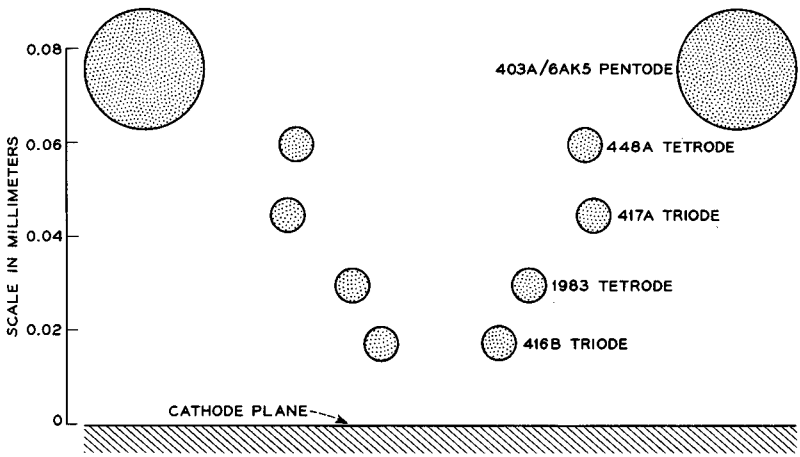

FIG. 7.4-4 The grid-wire diameter, the grid pitch, and the cathode-grid spacing for several tubes described in this chapter and in Chapter 5 are compared. Only two grid wires from each code are shown.

Figure 7.4-4 shows a comparison of the cathode-grid spacing used in this tube and in several tubes described earlier. The cross section of two grid wires from each tube are shown in relation to a common "cathode plane." The 416B has the same cathode area as the 1983, but a smaller cathode-grid spacing.

Several factors bearing upon the choice of grid-anode spacing in the 416B are:

1. The bandwidth $G_o/2\pi C_o$ can be increased by increasing the grid-anode spacing and hence reducing C_o.

2. Increasing the grid-anode spacing with a fixed anode voltage increases the transit angle for the grid-anode region and reduces the power gain.

3. Increasing the anode voltage to reduce the transit angle in the grid-anode region increases the power dissipation in the envelope structure. In practice, the permissible anode dissipation is limited to about 6 watts because of the proximity of the metal-glass seal which joins the anode terminal to the glass ring that surrounds it.

4. Increasing the grid-anode spacing with a fixed anode voltage requires a higher average voltage at the grid plane in order to draw the required cathode current density and total anode current. However, the peak grid voltage cannot be permitted to go very far positive, or the grid interception would become excessive.

In practice the highest possible anode voltage is used consistent with the power handling capabilities of the envelope structure. This permits a reasonably large grid-anode spacing with not too large a transit angle (92 degrees at 4000 Mc/sec) and without excessive grid interception. Forced-air cooling of the anode is used to help conduct away the 6 watts of power dissipated in the anode by the electron beam.

The 416B is used in a three-stage amplifier which provides a small-signal power gain of 9db per stage at a midband frequency close to 4000 Mc/sec. The 3-db bandwidth of a single stage is 100 Mc/sec. As the input signal is increased from zero, the power gain at 4000 Mc/sec remains nearly constant up to a power output of about 20 milliwatts. However, at higher power outputs, the power gain falls with increasing power output; and at a power output of 0.5 watt, the midband power gain of the output stage is reduced to 5db.

PROBLEM

1. The beam of a cathode-ray tube passes between two parallel deflection plates of length d in the direction of the electron motion. Show that for small deflections of the beam by an *ac* signal applied to the deflection plates, the amplitude of the deflection is proportional to the beam coupling coefficient $\frac{\sin(\omega T_o/2)}{\omega T_o/2}$, where T_o is the time the electrons spend in traveling the distance d, and ω is the angular frequency of the *ac* signal applied to the plates. Assume that edge effects at the deflection plates can be neglected and that the field between the plates is uniform at any instant.

REFERENCES

7a. F. B. Llewellyn and L. C. Peterson, *Proc. IRE* **32**, 144, 1944.

7b. F. B. Llewellyn, *Electron Inertia Effects*, Cambridge University Press, Cambridge, England, 1943.

7c. J. A. Morton and R. M. Ryder, *Bell System Tech. J.* **29**, 496, 1950.